JMEPEG
https://doi.org/10.1007/s11665-021-05903-0

1059-9495/$19.00

Cold-Plasma-Sterilized Nanostructured Ti6Al4V: Effect on Nanostructured Surface Morphology and Osteogenic Differentiation of Bone-Marrow-Derived Mesenchymal Stem Cells

Leonardo Marasca Antonini, Antonio Shigueaki Takimi, Vanessa Pinheiro Amaral, Melissa Camassola, and Célia de Fraga Malfatti

Submitted: 5 March 2021 / Revised: 20 April 2021 / Accepted: 7 May 2021

The cold plasma sterilization is an alternative sterilization process that does not modify the morphological properties of nanostructured surfaces of titanium and its alloys. This study aims to evidence the effect of surface morphology of the cold-plasma-sterilized nanostructured Ti6Al4V on the osteogenic differentiation of bone marrow-derived mesenchymal stem cells (BM-MSCs). The surface treatments on Ti6Al4V used were sanding and electropolishing in a H_2SO_4/HF/glycerin solution. The samples were characterized by AFM, optical interferometry, and wettability. BM-MSCs were cultured for 14 days and tested for cell adhesion, metabolic activity, ALP activity, and mineralization. Results demonstrated that the nanostructured morphology of Ti6Al4V remained intact after the sterilization and promoted a more hydrophilic surface, which contributed to the increase in the metabolic activity, and to osteogenesis of BM-MSCs, as well as to the extracellular matrix mineralization. The bacteriological and mycological tests showed that bacteria, fungi, and yeasts were not detected after cold plasma sterilization.

Leonardo Marasca Antonini and **Célia deFraga?Malfatti**, LAPEC/PPGE3M, Universidade Federal do Rio Grande do Sul, Av. Bento Gonçalves, 9500, Prédio 43427, Sala 232, Porto Alegre, Rio Grande do Sul 91501-970, Brazil; **Antonio Shigueaki Takimi**, ELETROCORR/PPGE3M, Universidade Federal do Rio Grande do Sul, Av. Bento Gonçalves, 9500, Prédio 43427, Sala 216, Porto Alegre, Rio Grande do Sul 91501-970, Brazil; and **Vanessa Pinheiro Amaral** and **Melissa Camassola**, Programa de Pós-graduação em Biologia Celular e Molecular Aplicada à Saúde (PPGBioSaúde), Universidade Luterana do Brazil, Av. Farroupilha, São José, Canoas, Rio Grande do Sul 92425900, Brazil. Contact e-mail: leomantonini@gmail.com.

Journal of Materials Engineering and Performance

Published online: 03 June 2021

Graphical abstract

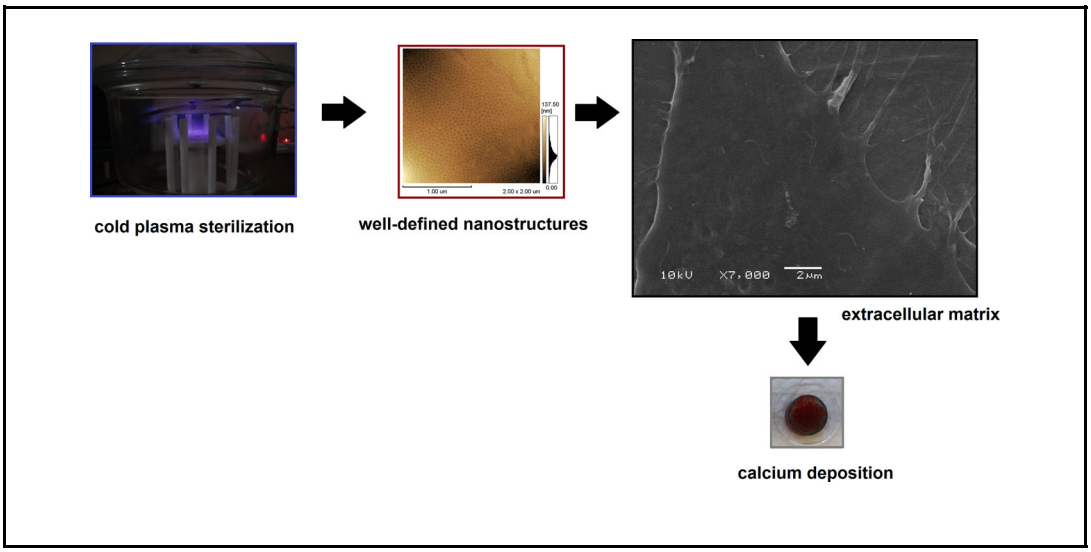

Keywords BM-MSCs, cold plasma sterilization, electropolishing, osteogenesis, Ti6Al4V

1. Introduction

Recently, alternative methods of sterilization have been employed aiming to replace traditional sterilization processes (Ref 1–3). Among alternative methods, cold plasma sterilization does not alter the morphological properties of titanium and its alloys (Ref 4). Cold plasma sterilization does not produce toxic by-products, is fast, and its cost is not high (Ref 5). As shown by Junkar et al. (Ref 6) when evaluating the effect of TiO_2 nanotubes in cytotoxicity tests, it was evidenced that the plasma sterilization process did not cause any changes in the morphology and chemical composition of the nanotubes. For Ueno et al. (Ref 7), the plasma sterilization process, in addition to not changing the morphology of biomaterials, has a high sterilization capacity. In their study, dental instruments contaminated with *Escherichia coli, Pseudomonas aeruginosa*, and *Staphylococcus aureus* had an effective elimination of the microorganisms, which were destroyed within 1-10 min of sterilization by cold plasma. During the sterilization process, the gas pressure was 13Pa in the discharge tube, 25Pa in the expansion chamber and 75mA discharge current. The temperature reached was 76 ° C for exposure in the expansion chamber and 80 ° C in the positive column.

A study developed by Nam et al. (Ref 8) showed that the cold plasma sterilization was suitable method in a clinical environment to eliminate the Escherichia coli, Staphylococcus aureus, and Saccharomyces cerevisiae deposited on a nitrocellulose filter membrane or Bacillus subtilis spores deposited on polypropylene. The plasma was generated with AC input power at 10 kHZ, 6kV, and after plasma treatment, the microorganisms were eliminated with 18 sec for *E. coli*, 19 sec for S. aureus, 1 min 55 sec for S. cerevisiae, and 14 min for B. subtilis spores.

Yu et al. (Ref 9) investigated the cold plasma sterilization in a population of 1.0×10^4-1.0×10^5 *Escherichia coli* or *Micrococcus luteus* bacteria. The complete kill of the *Micrococcus luteus* was less than 1 min exposures and about 2 min exposure for *Escherichia coli*. The cold plasma sterilization showed rapid sterilization capability, improving its sterilization efficacy through faster etching or erosion mechanisms of oxygen species.

Aiming to promote an improvement in the stem cell differentiation process, texturing methods have been used to obtain micropores or nanopores on titanium and its alloys, which tend to imitate the natural architecture of bone (Ref 10). Such structures can increase the cell-biomaterial interaction, allowing the transport of body fluid, increasing the growth of bone tissue, and facilitating vascularization (Ref 11). Nanostructured surfaces are able to increase the interaction of cells with the surface of biomaterials (Ref 12). Nanostructured surfaces can positively contribute to the process of stem cell differentiation (Ref 13). Nanotubes on the Ti6Al4V surfaces have favored the osteogenic differentiation of stem cells (Ref 14). Some studies using TiO_2 nanotube (Ref 15) and nanorod (Ref 16) arrays have been developed to promote the osteogenesis differentiation of mesenchymal stem cells (MSCs).

This study aims to evidence the sterilization efficiency and the effect of surface morphology of the cold-plasma-sterilized nanostructured Ti6Al4V on the osteogenic differentiation of bone marrow-derived mesenchymal stem cells (BM-MSCs). As previously reported by Antonini et al. (Ref 4), the cold plasma sterilization process does not cause changes in the nanometric and micrometric morphology of Ti6Al4V surfaces, contributing positively to the growth and differentiation of stem cells.

2. Material and Methods

2.1 Electrochemical Treatment

Titanium alloy (Ti6Al4V) disks with an exposed area of approximately 1.77 cm^2 and a thickness of 2 mm were used as substrate. All samples were initially manually polished by

abrading the samples using silicon carbide sandpapers until grit size 4000. Samples for electrochemical treatment were washed in deionized water using an ultrasonic bath and dried with cold air. They were electrochemically treated in an acidic solution consisting of sulfuric acid, hydrofluoric acid and glycerine in a 6:3:1 (v/v) ratio, using a DC power source (MPC-303DI, Minipa) with platinum as the cathode and the sample as the anode. The electrochemical treatment was carried out for either 4 or 12 min, 25V at 7 ° C ± 0.5 ° C.

After the electrochemical process, the electrochemically treated samples were washed again in an ultrasonic bath for 10 min.

2.2 Roughness and Wettability Analysis

The nanometric morphology and roughness were assessed by atomic force microscopy (AFM) (Ref 17) using a Shimadzu SPM - 9500J3 microscope (Shimadzu Corp., Kyoto, Japan), while the micrometric roughness was evaluated using a MITUTOYO SJ-400 profilometer (Mitutoyo America Corporation, Aurora, Illinois). Surface roughness (in micrometric scale) was determined by measuring the Ra (arithmetical mean of the absolute values within a sampling length), and the Rz (the vertical distance between the highest peak and the deepest valley within a sampling length). Nanometric roughness was obtained by measuring the Ra (arithmetical mean of the absolute values of the profile deviations from the mean line of the roughness profile) and the Rz (mean value of the sum of the height of the highest-profile of five peaks, and the depth of the deepest profiles valley, relative to the mean line, within a sampling length).

The surface wettability was determined by the sessile drop method using an equipment developed by the Corrosion Research Laboratory (LAPEC) at the Universidade Federal do Rio Grande do Sul (UFRGS, Porto Alegre, Brazil). With this equipment, it was possible to determine the contact angle between a drop of DMEM (Dulbecco's Modified Eagle's Medium from Sigma-Aldrich Co., LLC. Merck, Darmstadt, Germany) and the analyzed substrate. The contact angle was determined by image analyses using a SURFTENS 4.5 software (OEG, Frankfurt, Germany).

2.3 Cold Plasma Sterilization

The cold plasma sterilization was conducted with an RF plasma glow discharge, with maximum power of 65W and sterilizing time of 5 min in an atmosphere of N_2 and O_2 in the same proportion of the atmospheric air (78.1% N_2, 20.9% O_2, and 1% Ar) (Ref 18), at 250 μatm of pressure.

2.4 Microbiological assay

The assay to the detection of bacteriologic and micrologic growth was performed at Bacteriology Laboratory of the Veterinary Hospital of ULBRA. After cold plasma sterilization, the materials were inoculated in plate of Agar blood with 8% of sheep blood, in plates of MacConkey agar and BHI® (Brain Heart Infusion) and incubated at 37 ° C for 24 h. Agar Sabouraud was used to *Penicillium sp* fungal culture.

The bacterial colonies were identified from to colony morphology, presence or absence of hemolysis, lactose fermentation, gram stain, rapid tests (catalase, oxidase, coagulase), and indol tests, citrate, urea, sugar fermentation (glucose, sucrose, maltose, dulcitol, trehalose, mannose) VM/VP, SIM, and phenylalanine, as indicated by Cowan (Ref 19).

2.5 Cytotoxicity

Cell viability was tested by indirect contact using fibroblast cells (L929, BCR, batch no. 000604, Rio de Janeiro, Brazil) according to ISO 10993-5. The MTT test was performed in sextuplicate. Cells were incubated at 37 ° C and an atmosphere containing 5% CO_2. Cells (L929) were seeded in a 96-well tissue culture plate at a concentration of 10^4 cells/well (100 μL). After 24h, 48h, 72h, 7 days, and 14 days of contact between biomaterials and culture media (Dulbecco modified Eagle's medium—DMEM, Sigma, São Paulo), the media was added to wells with L929 cells and incubated for 24h at 37 ° C. Cells cultured with DMEM were used as negative control, and, as positive control, cells cultured with dimethyl sulfoxide (DMSO). A volume of 50μL of MTT (1 mg/mL) was added to each well. Formazan salts were dissolved in DMSO (100 μL), and the absorbance was measured at 570nm (Multiskan EX Microplate Reader, MTX Lab Systems, Vienna, USA). If the relative cell viability for the highest concentration of the sample extract (100% extract) is ≥ 70 % of control group, the material shall be considered non-cytotoxic.

2.6 Stem Cells Culture

This work step was performed at Tissue Engineering and Stem Cells Laboratory of the Lutheran University of Brazil. All reagents used in this study were from Sigma-Aldrich Co LLC unless otherwise stated. Plasticware was from BD Falcon (São Paulo, Brazil). Complete culture medium (10% v/v in CCM) was composed of Dulbecco's modified Eagle's medium supplemented with 10% fetal bovine serum (Gibco), 10 mM 4-(2-hydroxyethyl)-1-piperazine ethanesulfonic acid (HEPES), and 100 U penicillin mL-L and 10mg streptomycin mL-L solution (Gibco Invitrogen). Ca^{2+} - and Mg^{2+} -free Hank's balanced salt solution was used for washing tissues and cells. All experiments were made with cells in passages 4-6 and experimental triplicates. The use of stem cells in this work is associated with the differentiation capacity of these cells that can give rise to several cell types, including bone.

2.6.1 Isolation of Bone Marrow-Derived Mesenchymal Stem Cells (BM-MSCs). Bone marrow cells were harvested from the tibia and femur of 60-day-old female SHR rats. The bone marrow cavities of the rats were flushed with CCM (10% v/v). The cell layer was plated and cultured in CCM in 5% CO_2 at 37 ° C. The culture medium was replaced twice a week along with the removal of the non-adherent cells. When confluent, adherent cells (80-90%) were trypsinized and passaged onto a larger surface. Passage 4-6 cells were used for experiments. The use of these animals was approved by the Ethics Committee of FEPPS (MEMO n. 02/201, August 7, 2013).

2.6.2 Seeding of BM-MSCs onto the Materials. Before cell culture, all samples of biomaterial were sterilized by cold plasma generated from a radiofrequency discharge, maximum power of 65W and cleaning time of 5 min in an atmosphere of N_2 e O_2 in the same proportion of atmospheric air (78.1% N_2, 20.9% O_2 e 1% Argônio and other gases (Ref 18). After sterilization, the biomaterials were washed three times with PBS, orbitally shaking at 200 rpm for 20 min for each wash. Samples of biomaterial were seeded with 3×10^4cells/cm^2 and

allowed to attach on the surface for 45 min before submerging the disc in 2 mL of media and incubating overnight. On day 1, samples were transferred to a new well plate and 2 mL of media were added to selected samples. The media was changed every 2-3 days.

2.6.3 Cell Adhesion. The biomaterials used to cell adhesion assay were sanded titanium, mechanically polished Ti6Al4V, Ti6Al4V electropolished for 4 min, and Ti6Al4V electropolished for 12 min. BM-MSCs were seeded onto the biomaterials at 5×10^4 cells/cm^2 with CCM and incubated 90 min at 37 ° C with 5% of CO_2. Subsequently, constructs were washed to remove inadherent cells. The constructs were transferred to a new plate and incubated for three days. The plate containing inadherent cells were again incubated for 16h, stained with Giemsa, and the number of cells was directly counted. The results were expressed in the percentage of adhered cells.

2.6.3.1 Cell Spreading and Morphology. To examine the effects of the Ti6Al4V surface on cell spreading and morphology, cells attached on the samples that had been mechanically polished and electropolished for 4 or 12 min were observed using scanning electron microscopy (SEM; MIRA3, TESCAN, Brno, Czech Republic, operating at 10 kV and 15 kV). The samples were routinely prepared, dehydrated, and finally dried in a critical point dryer.

2.7 Cell Viability

The cells were maintained in contact with the biomaterials for 4 days, after that the cell viability was measured. Alamar blue assay was performed according to the manufacturer's instructions. Briefly, Alamar blue (Invitrogen; 10% v/v in CCM) was added to each well, and the plate was incubated for 3h. From which well, 100µL was transferred to 96-well plate and subsequently the measurements were carried out in a Spectramax M2 and fluorometer (Molecular Devices), using an excitation of 544m and an emission of 590nm. Data expressed as Fluorescence Intensity/10^4 cells plated.

2.8 Cell Differentiation

The osteogenic differentiation of bone marrow-derived mesenchymal stem cells was induced between passage three and five. $3x10^4$ cells/cm^2 were cultivated with specific media for 14 days and change of the culture media occurred every 3 days. For osteogenic differentiation, the complete culture media (CCM) was supplemented with 10^{-8}M dexamethasone, 5mg ascorbic acid 2-phosphate/mL, and 10mM de β-glycerophosphate. As control were used BM-MSCs plated in 24-well plates, for the same period, in CCM media and inducing media.

2.9 Alkaline Phosphatase Activity (ALP activity)

Alkaline phosphatase activity (ALP activity) is considered to reflect osteoblastic differentiation and plays a major role in bone formation and mineralization (Ref 20). The totals proteins were extracted in analyzed solution (300mM NaCl, 50mM Tris-HCl [pH 7.6], 0.1% TritonX-100, 200mM KCl, 0.5mM EDTA), and they were quantified by Bradford method (Bio-Rad, Richmond, CA, USA). The ALP activity was analyzed using the colorimetric conversion of p-nitrophenyl phosphate in p-nitrophenol product by 85L-2 kit (Sigma Aldrich).

Briefly, 20µL of total protein solution was incubated at 37 ° C in a 6.7mM solution of 4-Nitrophenylphosphate diluted in carbonate buffer (0.1 M) - $MgCl_2$ (2 mM) (pH 9.8). The test performed in a 96-well plate, in triplicate, with a total volume of 120 µL. A standard curve of p-Nitrophenol (product) diluted from 0.5 mM incubated on the same plate. A 0.2 M NaOH solution used to stop the reaction (final volume 200 µL). Alkaline phosphatase activity is expressed µM product/µg protein.

2.9.1 Mineralization. The osteogenic differentiation was performed for 3 and 11 days. Subsequently, the cells were fixed with 70% ethanol for 15 min and washed 3 times with distilled water. 1mL of Alizarin Red S (Sigma, São Paulo) was added to cells, and they were incubated for 30 min at room temperature. The excess of Alizarin corant was removed by washing with

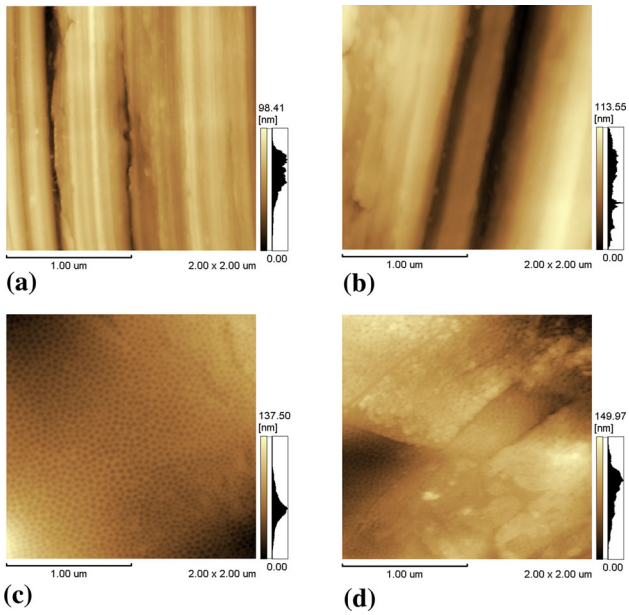

Fig. 1 AFM images of the studied samples. (a) Titanium, (b) Ti6Al4V, (c) Ti6Al4V Electr. Threat. 4 min, (d) Ti6Al4V Electr. Treat. 12 min

Table 1 Roughness values obtained on nanometric scale obtained by atomic force microscopy

Samples	Ra, nm	Rz, nm
Titanium	21 ± 0.2	73 ± 0.6
Ti6Al4V	24 ± 0.3	76 ± 0.5
Ti6Al4V electr. treat. 4 min	13 ± 0.4	31 ± 0.3
Ti6Al4V electr. treat. 12 min	19 ± 1	45 ± 1

Table 2 Roughness values obtained on micrometric scale obtained by contact profilometry

Samples	Ra, µm	Rz, µm
Titanium	0.1 ± 0.05	0.5 ± 0.03
Ti6Al4V	0.1 ± 0.04	0.7 ± 0.02
Ti6Al4V electr. treat. 4 min	0.2 ± 0.01	1.3 ± 0.2
Ti6Al4V electr. treat. 12 min	0.2 ± 0.01	1.8 ± 0.1

distilled water. The cells were then incubated with 500μL of isopropanol for 5 min. The samples were distributed on 96 wells to electro-spectrophotometric measuring (Multiskan Ex original, Serial RS-232c) using an optical density of 540nm. The mineralization was quantified from a molar ratio of 1:2 between Alizarin and calcium.

2.9.2 Statistical Analysis. All statistical analyses were undertaken in GraphPad Prism (version 7.00; GraphPad Software, Inc., San Diego, California). The cell growth and cell differentiation were evaluated using six samples per system. Depending on whether a response affected by one or two factors, either one- or two-way ANOVA with a Tukey's post-test was used to evaluate significant differences. All graphs presented as mean ± standard deviation and notable significant differences indicated on the graphs or in the legends.

3. Results and Discussion

3.1 Morphological and Physical-Chemical Characterization

The samples treated electrochemically for 4 min showed the formation of well-defined nanostructures (Fig. 1c) while in the electrochemically treated sample at 12 min the thickening of the oxide layer prevailed (Fig. 1d). The formation of nanostructures probably occurred because of the anodic dissolution process prevailing about the thickening behavior of the oxide layer, as reported by Antonini et al. (Ref 10). The grooves from the mechanical preparation of titanium and Ti6Al4V alloy are shown in the nanometric morphology of Fig. 1(a) and (b), respectively.

Table 1 shows the results of nanometric roughness, and it is observed that for the sanded samples only, the nanometric roughness values were higher than those observed for the samples treated electrochemically for 4 and 12 min. Regarding micrometric roughness values (Table 2), no significant difference was observed between average roughness values (Ra) for all systems studied, with values in the order of 0.1-0.2 μm. Because competition between anodic dissolution and thickening of oxide layer, the samples treated electrochemically for four and 12 min showed an increase in micrometric roughness compared to the only sanded samples.

Keller et al. (Ref 21) showed that the increase in implant roughness from texturing processes can improve cell adhesion and proliferation. While Zhu et al. (Ref 22) found that osteoblasts have a good affinity for surfaces with medium roughness (Ra) close to 0.5 μm. As shown by Zhu et al. (Ref 23), the osteoblast growth on titanium surfaces with less micrometric roughness had few cytoplasmic extensions, compared to surfaces with micro- and submicrometric roughness. This shows that cells not only feel the direction of the topography of the substrate but also respond to irregularities present in the morphology.

According to Bacakovz et al. (Ref 24), the surface roughness can be divided into macroroughness (>100 μm), microroughness (1-100 μm), submicron roughness (100 nm-1 μm), and nanoroughness (<100 nm). Li et al. (Ref 25) have described that surfaces with micro-roughness positively aid in cell proliferation and differentiation. Surfaces with nanoroughness allow better osseointegration; the authors believe that surfaces with roughness less than 100 nm can mimic a nanoarchitecture of natural tissues (Ref 26). The cells can show different responses to different surface morphologies such as grooves (Ref 27), tubes (Ref 28), meshes (Ref 29), or columns (Ref 30). Deng et al. (Ref 26) have highlighted that surfaces with nanometric roughness improve cell differentiation and proliferation, Olivares-Navarrete et al. reported that better results are obtained with micro-rough surfaces (Ref 31). The authors showed that differentiation in osteoblastic cells increased with the presence of Ti6Al4V nanostructured surfaces (Ref 32). A study by Deng et al. showed that nanostructured titanium contributed positively to the adhesion, viability, and differentiation of stem cells (Ref 26).

Contact angle measurements in DMEM and H_2O after cold plasma cleaning of samples are shown in Table 3. From these results, it was possible to observe low values of contact angle in the samples treated electrochemically for 4 min compared to the samples treated electrochemically for 12 min and samples sanded in both DMEM and H_2O. The decrease in the contact angle for the electrochemically treated samples for 4 min may have been influenced by the anodic dissolution predominantly concerning the formation and thickening of the oxide layer observed in the electrochemically treated sample for 12 min. As shown by Antonini et al. (Ref 33) air plasma cleaning results in superficial cleaning in which functional groups adsorbed on the surface are removed, this removal prevents interaction with dexamethasone proteins (a substance present in the osteogenic medium), and for this reason, the effect of nanometric roughness (nanotexturization) and wettability is more easily perceived by cells. Bárdos et al. (Ref 34) observed an increased surface energy (decreased contact angle) after plasma treatment, which resulted in an improve adhesion on surface and coatings.

Cunha et al. (Ref 35) investigated the wetting behavior of Ti6Al4V alloy surfaces textured, and they showed that the treated surfaces presented contact angles much smaller than polished surface and that the surface topography plays an important role in controlling wettability. The authors explain that the air tends to get stuck in the irregularities of the surface and this behavior contributes to the decrease in wettability. Moreover, the surface topography seems to affect the surface wetting more than its own roughness. While Cui et al. (Ref 36) evaluated the surface characteristics of Ti8Ta3Nb alloy compared to TiS and Ti6Al4V alloy on osteoblastic response, they observed that micrometric roughness and morphology were similar to all samples. Moreover, the wettability measurements showed water contact angle values of TiS, Ti6Al4V, and Ti8Ta3Nb alloy 66°, 70°, and 63°, respectively, and the greater hydrophilicity of the surface was related to TiOH groups.

Table 3 Contact angle measurements in DMEM and H_2O obtained by the wettability technique

Samples	DMEM, °	H_2O, °
Titanium	79 ± 0.5	63 ± 2
Ti6Al4V	85 ± 0.2	70 ± 3
Ti6Al4V electr. treat. 4 min	57 ± 1	40 ± 2
Ti6Al4V electr. treat. 12 min	74 ± 2	47 ± 0.4

3.2 Biological Assays

Here, the results of the tests of association of biomaterials with bone marrow-derived mesenchymal stem cells (BM-MSCs) will be presented from contact with biomaterials

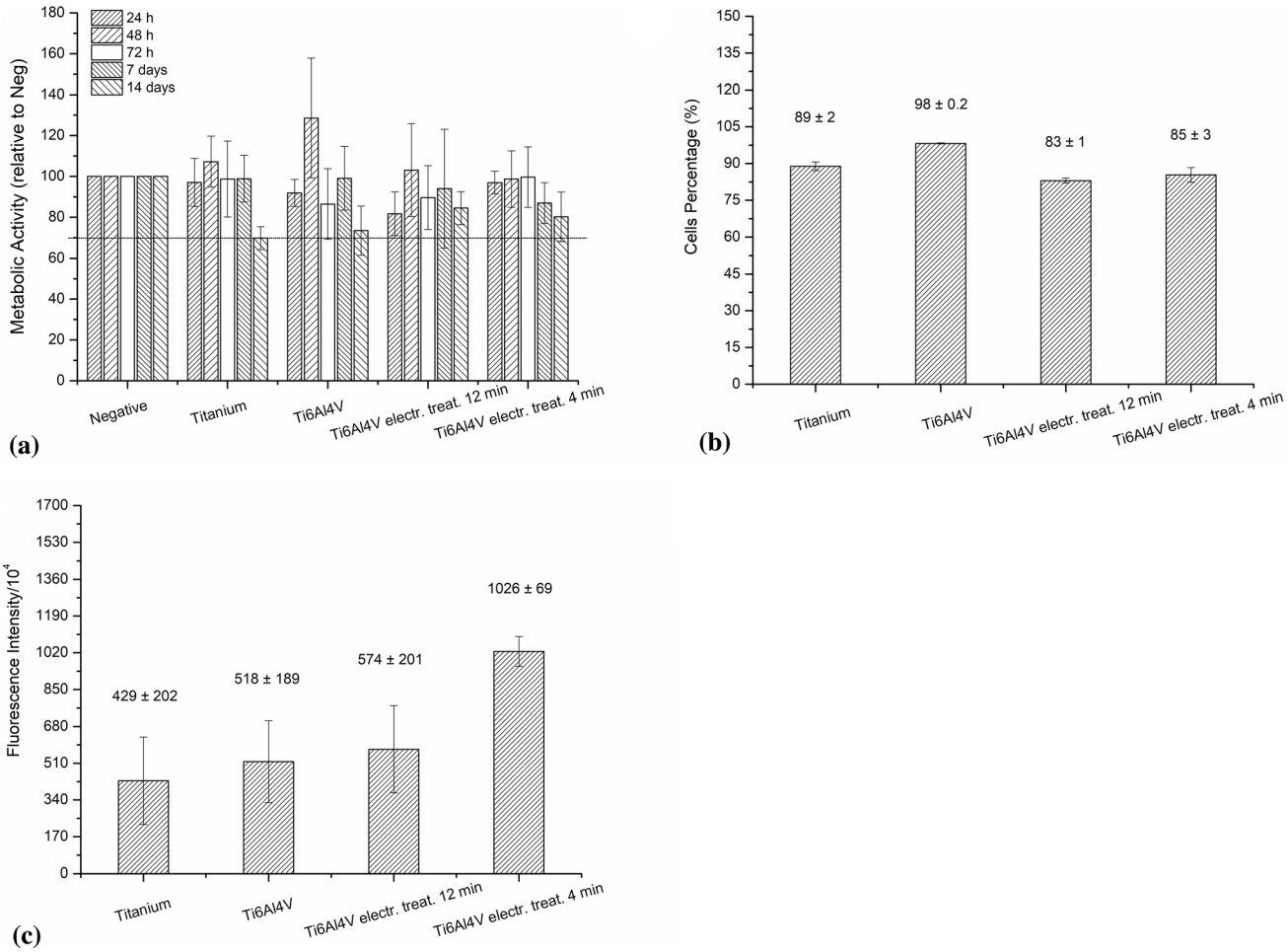

Fig. 2 Evaluation of the effect of contact between BM-MSCs and biomaterials. (a) Cytotoxicity after 24h, 48h, 72h, 7 days and 14 days of exposure to the extract of biomaterials, (b) Cell adhesion for all evaluated biomaterials. $*p < 0.005$, $**p < 0.0005$, $***p < 0.003$, $****p < 0.01$ and (c) Cell viability of BM-MSCs after 4 days of contact with biomaterials. $*p < 0.008$, $**p < 0.01$, $***p < 0.02$

sterilized by air plasma (pure Ti, Ti6Al4V, Ti6Al4V electrochemically treated for 4 and 12 min). Such results come from the bacteriological and mycological assay, cytotoxic potential, cell adhesion, proliferation of BM-MSCs, and cell differentiation in osteogenic medium, with dosages of alkaline phosphatase and calcium deposition (bone matrix deposition).

3.2.1 Microbiological Assay. Among the sterilization methods employed (Cold plasma, Ethanol + PBS, and Autoclave), the cold plasma sterilization method did not change the morphology of the electrochemically treated surfaces for 4 min; besides, it did not change the values of nanometric roughness and micrometric roughness, making the surface more hydrophilic after sterilization; this method was chosen for tests with bacteria (bacteriological) and fungi or yeasts (mycological).

According to the bacteriological test, there was no bacterial growth and with the mycological test, there was no growth of fungi and/or yeasts. Therefore, the results of the bacteriological and mycological tests showed that the cold plasma sterilization method was efficient, sterilizing the surface since the presence of bacteria or fungi/yeasts on the surface was not detected after sterilization.

3.2.2 Cytotoxic Potential, Cell Adhesion, and Viability. In Fig. 2, the results of cytotoxicity for all systems showed that none of the systems was cytotoxic at 3 days of testing (72 h), according to ISO 10993-5: 2009. However, after 14 days of contact between biomaterials and media, the extract of pure titanium was the only group that showed a tendency to present cytotoxic behavior. This behavior may be related to the presence of debris present on the surface from mechanical sanding, decreasing cell viability, and favoring the appearance of a structure similar to apoptosis, as already indicated by Wang et al. (Ref 37).

Wang et al. (Ref 37) showed that the osteogenic differentiation of mesenchymal stem cells derived from human marrow stroma was impaired by titanium particles exposed on the surface; reducing cell viability and proliferation. The authors showed that the exposure of titanium particles from surface wear compromised cell viability, consequently inducing apoptosis. For Wang et al. (Ref 38), the exposure of these titanium particles from some type of superficial wear contributes to the reduction in bone formation and compromises osseointegration at the implant/bone interface. After 24h and 72h, cells exposed to titanium particles exhibited high levels of cytotoxicity, while in shorter exposure time (6h) the particles did not show a cytotoxic effect.

Authors such as Ortega et al. (Ref 39) studied the cytotoxicity of Ti6Al4V from an aluminum oxide sandblasting process and a nitric acid passivation process in rat L929 fibroblasts and human MRC-5 fibroblasts and found no cytotoxic behavior against the evaluated surfaces. The authors

also showed that Ti6Al4V did not induce mutagenic effects when in contact with *E. coli*. Rae (Ref 40) performed the incubation of human synovial fibroblasts for 8 days on Ti6Al4V but did not show cytotoxicity, besides, the presence of significant amounts of vanadium, titanium, and aluminum dissolved from the alloy was not detected.

According to Esposito et al. (Ref 41), alloys such as Ti6Al4V contain aluminum in their composition, and according to the authors, this causes a layer of aluminum oxide to form on the surface which can exert some cytotoxic effect. Okazaki et al. (Ref 42) studied the cytotoxic effect of several metal ions on L929 fibroblasts and MC3T3-E1 osteoblasts, with no cytotoxic effect of Ti, Zr, Sn, Nb, and Ta; however, the ions of Al and V exhibited cytotoxicity from concentrations above or equal to 0.2ppm, and the cytotoxic effect of Al was more pronounced on cells in media containing the amount of V ions below 0.03ppm.

Figure 2(b) shows the results of cell adhesion expressed as % of cells adhered to the evaluated biomaterials, observing that all biomaterials showed cell adhesion. The only sanded samples of Ti6Al4V showed greater cell adhesion than the other biomaterials, but similar adhesion results were found among the samples treated electrochemically for 4 and 12 min.

In Fig. 2(c), the cell viability results of BM-MSCs are presented after 4 days of cultivation with the sanded pure Ti, sanded Ti6Al4V, electrochemically treated Ti6Al4V systems for 4 min, and electrochemically treated Ti6Al4V for 12 min.

These results indicate that in the Ti6Al4V sample system treated electrochemically for 4 min, the cells showed greater cell viability than in other biomaterials. This increase may have been favored by the nanostructured surface without the presence of regions with thickening of the oxide layer and by the fact that this surface was sterilized by cold plasma, which contributed to the increase in hydrophilicity. Huang et al. (Ref 43) showed that changes in the nanotopography of electrochemically treated Ti6Al7Nb samples improved cell adhesion and proliferation. The same authors indicated that a nanoscale oxide layer on the surface of the Ti6Al7Nb alloy improved its biocompatibility.

Sista et al. (Ref 44) evaluated the adhesion of MC3T3-E1 osteoblasts from rodents to the Ti-Zr alloy and observed that cell adhesion was greater on those surfaces with nanotubes and with greater nanometric roughness than on those surfaces that were only mechanically polished. Partida et al. (Ref 45) showed that the adhesion and cell viability of osteoblasts were increased on the nanostructured surfaces of Ti6Al4V, present-

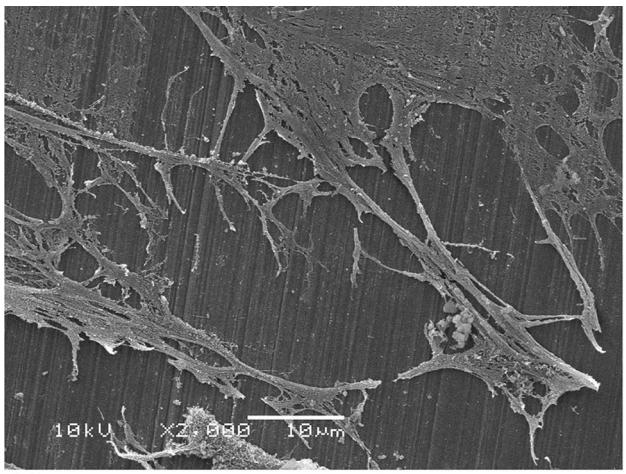

(a)

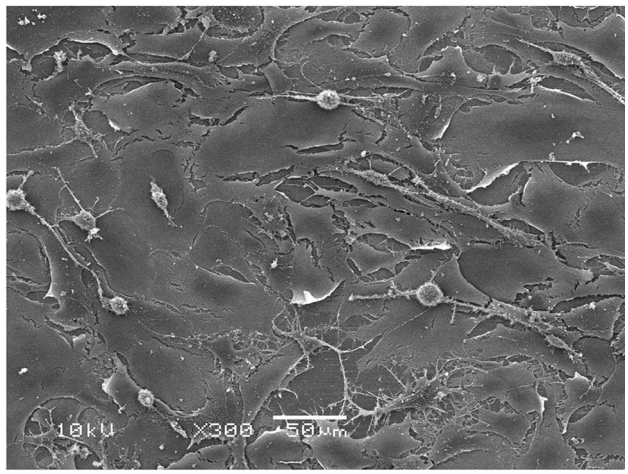

(b)

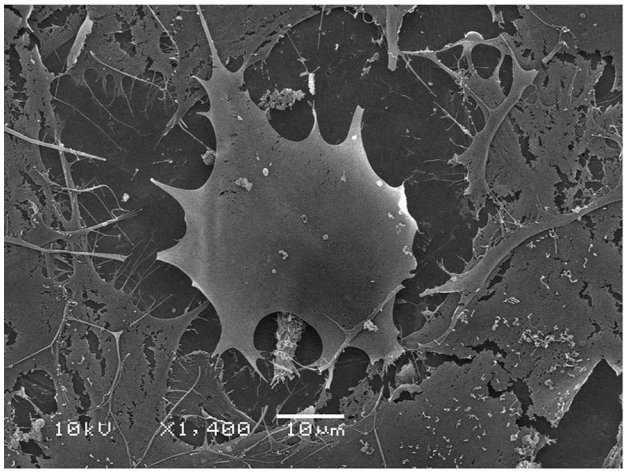

(c)

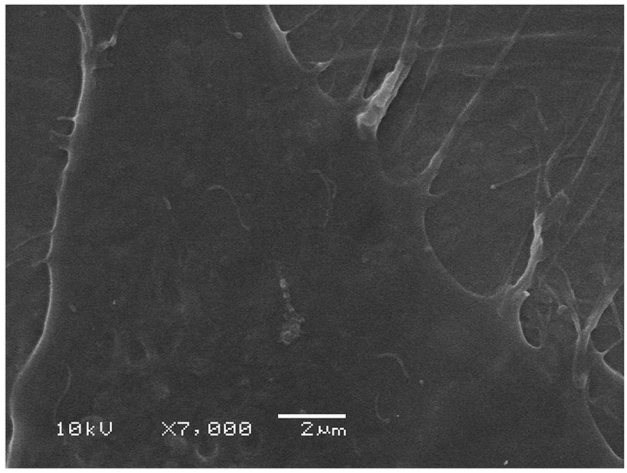

(d)

Fig. 3 SEM images of samples after 4 days of BM-MSC culture test: Titanium (a), Ti6Al4V (b), Ti6Al4V electrochemically treated for 12 min (c), Ti6Al4V electrochemically treated for 4 min (d)

ing a greater number of cellular interconnections and an increase in the number of cellular philopodia anchored on the nanostructures. Stan et al. (Ref 46) observed a greater growth of G292 osteoblasts on TiO_2 nanotubes in Ti6Al4V when compared to anodized Ti6Al7Nb alloy.

A study realized by Han et al. (Ref 47) showed that the plasma-treated titanium surface had an increase in surface energy and it promoted an increase in cell adhesion and proliferation. This behavior may be related to the explanation produced by Williams et al. (Ref 48), which indicated that the plasma treatment can eliminate the hydrocarbon contaminants from the surface, followed by the chemical functionalization of the metal oxide, in addition to increasing the surface energy. For Moreira et al (Ref 49), plasma treatment promoted the inactivation of microorganisms, minimizing damage to the surface of materials.

Figure 3 shows SEM images of biomaterials after cell adhesion and culture for 4 days. SEM images of pure Ti biomaterials (Fig. 3a), sanded Ti6Al4V (Fig. 3b) and Ti6Al4V electrochemically treated for 12 min (Fig. 3c) corroborate the results obtained from cell viability (Fig. 2c), and it is possible to visualize by the SEM images the proliferation of cells of polygonal geometry and the formation of a fragmented extracellular matrix.

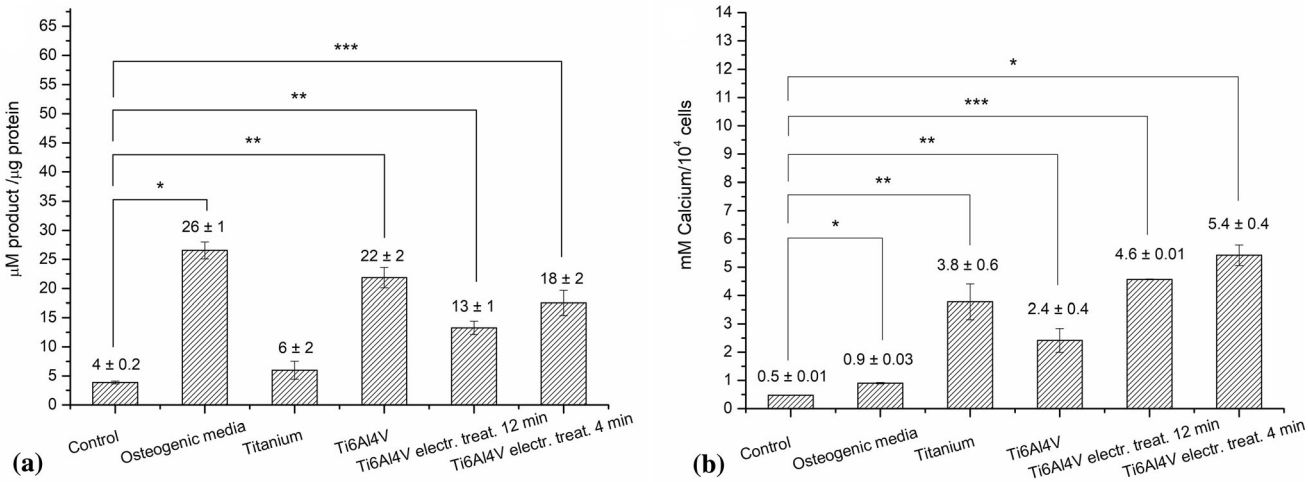

Fig. 4 Quantification of osteogenic differentiation markers. (a) Alkaline phosphatase activity expressed in μM product / μg protein (n = 3). *$p < 0.000002$, **$p < 0.0001$, ***$p < 0.0003$ e (b) Indirect quantification of mineralization expressed in Mm of calcium/10^4 cells. *$p < 0.00003$, **$p < 0.001$, ***$p < 0.0001$

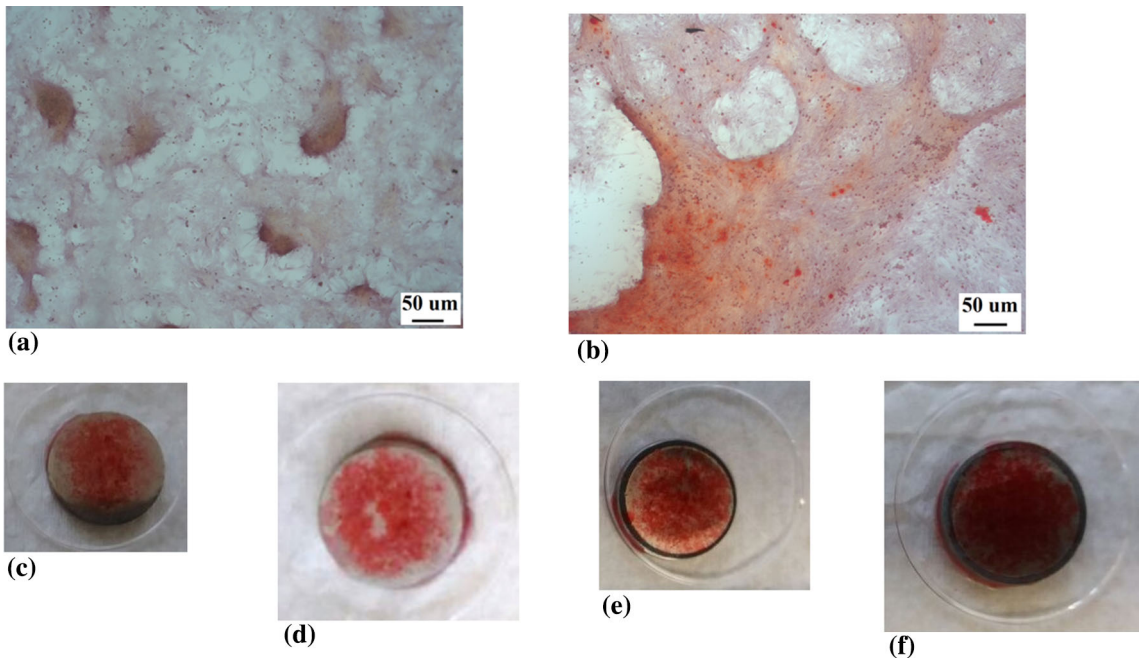

Fig. 5 Images showing the surface of the samples after the Alizarin Red Stain (Bone matrix deposition). (a) BM-MSCs kept in CCM medium, (b) BM-MSCs maintained in osteogenic medium, (c) BM-MSCs associated with pure titanium in osteogenic medium, (d) BM-MSCs associated with Ti6Al4V in osteogenic medium. Scale bar: 50 μm, increase: 10x. (e) BM-MSCs associated with Ti6Al4V electrochemically treated for 12 min in osteogenic medium and (f) BM-MSCs associated with electrochemically treated Ti6Al4V for 4 min in osteogenic medium

On the Ti6Al4V sample treated electrochemically for 4 min (Fig. 3d), the formation of an intact extracellular matrix without regions of fragmentation and rupture of cytoplasmic extensions is visualized. The formation of this extracellular matrix is one of the indications that the nanostructures obtained after 4 min of electrochemical treatment contributed significantly to the adhesion of cells on the surface, promoting cell proliferation and subsequent formation of the extracellular matrix. Some authors have reported that surface treatment in Ti6Al4V can contribute to cell growth and adhesion, as observed by Wang et al. (Ref 50) bone marrow-derived mesenchymal stem cells fully extended over Ti6Al4V surfaces with surface treatment by electron beam fusion (EBM) and selective laser fusion (SLM); also the cells showed high cell density and exhibited philopody (cytoplasmic extensions) after 24h of cell culture. These results showed that all Ti6Al4V samples treated by EBM and SLM showed good cell adhesion and that the evaluated samples showed good cytocompatibility. In the same sense, Han et al. (Ref 51) cultured bone marrow-derived mesenchymal stem cells on Ti6Al4V nanotubes, and they realized that the cells had a rounded shape, with long extensions and abundant lamellipodia; also, the authors noticed the formation of an extracellular matrix (ECM) deposited on the Ti6Al4V nanotubes.

Besides, in Fig. 3(a) there is adhesion of the cells through the filopodia (cytoplasmic extensions) in the grooves obtained by the mechanical sanding of the titanium. This shows that the roughness contributed significantly to cell adhesion and subsequent proliferation.

Although it is possible to visualize an extracellular matrix in the sample of Ti6Al4V only sanded, it is easy to visualize regions indicating apoptosis of the cells, as Fig. 3(b).

3.2.3 Cell Differentiation and Mineralization. In Fig. 4, the results of alkaline phosphatase activity in osteogenic medium for all biomaterials evaluated are presented. From the ALP values in μM of product/μg of protein (Fig. 4a), it is possible to verify that while the cells on pure Titanium showed slower cell differentiation, in the Ti6Al4V alloy there was an acceleration of cell differentiation. This behavior is inversely related to what is being presented in the results of calcium deposition (mineralization) (Fig. 4b), it is possible to see that on Ti6Al4V the deposition of calcium was lower than on pure Ti.

According to Stein et al. (Ref 52), cells may show slower cell differentiation due to the mineralization process taking place since normally the mineralization process starts when the differentiation stage is completed.

Regarding the Ti6Al4V samples treated electrochemically for 4 and 12 min, it appears that the cell differentiation step (Fig. 4a) was faster and calcium deposition (Fig. 4b) was higher for the electrochemically treated sample for 4 min. This shows that such processes are occurring faster on the electrochemically treated sample for 4 min than on the electrochemically treated sample for 12 min. The presence of nanostructures, in addition to the greater wettability of the electrochemically treated sample for 4 min, may have contributed significantly to accelerate cell differentiation, increasing the mineralization stage (calcium deposition). According to Mozetic et al. (Ref 53), the hydrophilicity/hydrophobicity should be explored, because it improves the materials response in biological environments.

Figure 5 presents the samples after Alizarin assay, which makes visible the deposition of bone matrix (indicated by the reddish color) allowing to affirm that the cells differentiated for all biomaterials.

Brammer et al. (Ref 54) studied the presence of osteoblasts on TiO_2 nanotubes on titanium substrate and showed an increase in ALP activity levels after cell contact on TiO_2 nanotubes, besides, the authors indicated that there was an increase in elongated philopodia.

The sanded Ti6Al4V sample showed faster cell differentiation compared to electrochemically treated samples for 4 and 12 min (Fig. 4a), and this behavior may be related to higher average nanometric roughness (Ra); since for the sanded sample Ra was 24nm and for the electrochemically treated samples, the Ra was around 13-19nm, as shown in Table 1.

Boyan et al. (Ref 55) have shown that osteoblastic cells on rougher titanium surfaces tend to increase ALP (cell differentiation) activity. B. D. Boyan et al. (Ref 56) showed that the growth of osteoblasts on a micro-rough surface produces an osteogenic environment capable of promoting osteoblastic differentiation through paracrine and autocrine communication among cells.

4. Conclusions

The cold plasma sterilization is presented as an efficient method to sterilize the metallic surface. The Ti6Al4V electropolished for four min showed faster formation of nanostructures and greater wettability than the other evaluated surfaces. None of the evaluated biomaterials was cytotoxic after 72 h of cytotoxic assay, proving that the electrochemical treatments performed on the surface of the biomaterials and cold plasma sterilization were not harmful to stem cells. The nanostructured surface of Ti6Al4V sterilized by cold plasma promoted an increase in cell growth in osteogenic medium and a greater number of adhered cells, in addition to an increased capacity for cell differentiation and mineralization. The cold plasma sterilization process associated with nanostructured morphology contributed significantly to a better cellular response since in previous works it has been reported that conventional sterilization methods, such as ethanol + PBS sterilization (Ref 4) and sterilization by autoclave (Ref 10) altered morphological properties and negatively affected stem cell growth.

Acknowledgments

The present work was carried out with the support of CAPES (Brazilian Coordination for the Improvement of Higher Education Personnel) (CAPES - PROEX Process 23038.000341/2019-71), CNPq (National Council for Scientific and Technological Development) [Grants No. 408366/2018-4] and FAPERGS [Grants Nos. 19/2551-0002280-8 and 19/2551-0000699-3]. Célia de Fraga Malfatti acknowledges CNPq (Grant 307723/ 2018-6). L.M. Antonini thanks for the postdoctorate scholarship CAPES PNPD (Grant PNPD20132547). The authors would like to thank Jane Brazil (from Universidade Luterana do Brasil - ULBRA, Brazil), for her technical services related to cell culture. INCT-Regenera. All authors certify that they have no affiliations with or involvement in any organization or entity with any financial interest or non-financial interest in the subject matter or materials discussed in this manuscript.

Authors Contribution

LMA contributed to investigation, writing, methodology—original draft. VPA contributed to methodology, investigation, writing—review. MC contributed to writing—review. AST contributed to conceptualization, formal analysis. CFM contributed to conceptualization, supervision, formal analysis.

Funding

This research did not receive any specific grant from funding agencies in the public, commercial, or not-for-profit sectors.

Conflict of interest

The authors indicated no potential conflicts of interest.

References

1. X.L. Liu, W.R. Zhou, Y.H. Wu, Y. Cheng and Y.F. Zheng, Effect of Sterilization Process on Surface Characteristics and Biocompatibility of Pure Mg and MgCa Alloys, *Mat. Sci. Eng. C*, 2013, **33**, p 4144–4154. https://doi.org/10.1016/j.msec.2013.06.004
2. Y. Zhao, B. Zhu, Y. Wang, C. Liu and C. Shen, Effect of Different Sterilization Methods on the Properties of Commercial Biodegradable Polyesters for Single-Use, Disposable Medical Devices, *Mat. Sci. Eng. C*, 2019, **105**, p 110041–110049. https://doi.org/10.1016/j.msec.2019.110041
3. S.A. Smith, B. Gause, D. Plumley and M.J. Drexel, Irradiation-Assisted Stress-Corrosion Cracking of Nitinol During eBeam Sterilization, *J. Mater. Eng. Perform.*, 2012, **21**, p 2638–2642. https://doi.org/10.1007/s11665-012-0396-8
4. L.M. Antonini, C.F. Malfatti, G.C. Reilly, R. Owen and A.S. Takimi, Effect of Sterilization Processes on Nanostructured Ti6Al4V Surfaces Obtained by Electropolishing, *J. Mater. Res.*, 2019, **34**(8), p 1439–1446. https://doi.org/10.1557/jmr.2019.28
5. M.M. Rodrigues, C.P. Fontoura, C.S.C. Garcia, S.T. Martins, J.A.P. Henriques, C.A. Figueroa, M.R. Ely and C. Aguzzoli, Investigation of Plasma Treatment on UHMWPE Surfaces: Impact on Physicochemical Properties, Sterilization and Fibroblastic Adhesion, *Mat. Sci. Eng. C*, 2009, **102**, p 264–275. https://doi.org/10.1016/j.msec.2019.04.048
6. I. Junkar, M. Kulkarni, B. Drasler, N. Rugelj, A. Mazare, A. Flasker, D. Drobne, P. Humpolícek, M. Resnik, P. Schmuki, M. Mozetic and A. Iglic, Influence of Various Sterilization Procedures on TiO_2 Nanotubes used for Biomedical Devices, *Bioelectrochemistry*, 2016, **109**, p 79–86. https://doi.org/10.1016/j.bioelechem.2016.02.001
7. M. Ueno, W.M.I. Urruchi, A.O.C. Jorge, C. Otani and H.S. Maciel, Esterilização de Limas Endodônticas com Plasma de Oxigênio, *Pesqui. Odontol. Bras.*, 2000, **14**(3), p 205–208. https://doi.org/10.1590/S1517-74912000000300003
8. K. Lee, K. Paek, W. Tae and Y. Lee, Sterilization of Bacteria, Yeast, and Bacterial Endospores by Atmospheric-Pressure Cold Plasma using Helium and Oxygen, *J. Microbiol.*, 2006, **44**(3), p 269–275
9. Q.S. Yu, C. Huang, F.H. Hsieh, H. Huff and Y. Duan, Sterilization Effects of Atmospheric Cold Plasma Brush, *Appl. Phys. Lett.*, 2006, **88**(3), p 013903-1-013903–3. https://doi.org/10.1063/1.2161807
10. L.M. Antonini, V. Kothe, G.C. Reilly, R. Owen, J.S. Marcuzzo and C.F. Malfatti, Effect of Ti6Al4V Surface Morphology on the Osteogenic Differentiation of Human Embryonic Stem Cells, *J. Mater. Res.*, 2017, **32**(20), p 3811–3821. https://doi.org/10.1557/jmr.2017.392
11. A. Tavangar, B. Tan and K. Venkatakrishnan, Synthesis of Bio-Functionalized Three-Dimensional Titania Nanofibrous Structures Using Femtosecond Laser Ablation, *Acta Biomater.*, 2011, **7**(6), p 2726–2732. https://doi.org/10.1016/j.actbio.2011.02.020
12. B.-S. Moon, S. Kim, H.-E. Kim and T.-S. Jang, Hierarchical Micro-Nano Structured Ti6Al4V Surface Topography via Two-Step Etching Process for Enhanced Hydrophilicity and Osteoblastic Responses, *Mat. Sci. Eng. C*, 2017, **73**, p 90–98. https://doi.org/10.1016/j.msec.2016.12.064
13. X. Liu and S. Wang, Three-Dimensional Nano-Biointerface as a New Platform for Guiding Cell Fate, *Chem. Soc. Rev.*, 2014, **43**(8), p 2385–2401. https://doi.org/10.1039/C3CS60419E
14. E. Filova, J. Fojt, M. Kryslova, H. Moravec, L. Joska and L. Bacakova, The Diameter of Nanotubes Formed on Ti-6Al-4V Alloy Controls the Adhesion and Differentiation of Saos-2 Cells, *Int. J. Nanomed.*, 2015, **10**, p 7145–7163. https://doi.org/10.2147/IJN.S87474
15. J. Park, S. Bauer, A. Pittrof, M.S. Killian, P. Schmuki and K. von der Mark, Synergistic Control of Mesenchymal Stem Cell Differentiation by Nanoscale Surface Geometry and Immobilized Growth Factors on TiO_2 Nanotubes, *Small*, 2012, **8**(1), p 98–107. https://doi.org/10.1002/smll.201100790
16. J. Qiu, J. Li, S. Wang, B. Ma, S. Zhang, W. Guo, X. Zhang, W. Tang, Y. Sang and H. Liu, TiO2 Nanorod Array Constructed Nanotopography for Regulation of Mesenchymal Stem Cells Fate and the Realization of Location-Committed Stem Cell Differentiation, *Small*, 2016, **12**(13), p 1770–1778. https://doi.org/10.1002/smll.201503946
17. Y. Kutes, V. Vyas and B.D. Huey, Nano and Micro Scale Analysis of Dentin with in vitro and High Speed Atomic Force Microscopy, *J. Mater. Res.*, 2013, **28**(17), p 2300–2307. https://doi.org/10.1557/jmr.2013.159
18. M. Pidwirny, Atmospheric composition: fundamentals of physical geography, 2nd ed., National Council of Educational Research and Training, 2006 (New Delhi)
19. R.K.A. Feltham and G.I. Barrow, *Cowan and Steel's Manual for the Identification of Medical Bacteria*, 2nd ed. Cambridge University Press, Cambridge, 1993
20. C.D. Hoemann, H. El-Gabalawy and M.D. McKee, In vitro Osteogenesis Assays: Influence of the Primary Cell Source on Alcaline Phosphatase Activity and Mineralization, *Pathol. Biol.*, 2009, **57**(4), p 318–323. https://doi.org/10.1016/j.patbio.2008.06.004
21. J.C. Keller, G.B. Schneider, C.M. Stanford and B. Kellogg, Effects of Implant Microtopography on Osteoblast Cell Attachment, *Implant Dent.*, 2003, **12**(2), p 175–181. https://doi.org/10.1097/01.ID.0000058309.77613.87
22. X. Zhu, J. Chen, L. Scheideler, R. Reichl and J. Geis-Gerstorfer, Effects of Topography and Composition of Titanium Surface Oxides on Osteoblast Respondes, *Biomaterials*, 2004, **25**, p 4087–4103. https://doi.org/10.1016/j.biomaterials.2003.11.011
23. X. Zhu, J. Chen, L. Scheideler, T. Altebaeumer, J. Geis-Gerstorfer and D. Kem, Cellular Reactions of Osteoblasts to Micron- and Submicron-Scale Porous Structures of Titanium Surfaces, *Cells Tissues Organs*, 2004, **178**(1), p 13–22. https://doi.org/10.1159/000081089
24. L. Bacakova, E. Filova, M. Pariek, T. Ruml and V. Svorcik, Modulation of Cell Adhesion, Proliferation and Differentiation on Materials Designed for Body Implants, *Biotechnol. Adv.*, 2011, **29**(6), p 739–767. https://doi.org/10.1016/j.biotechadv.2011.06.004
25. H.F. Li, Y.B. Wang, Y.F. Zheng and J.P. Lin, Osteoblast Response on Ti- and Zr-based Bulk Metallic Glass Surfaces after Sand Blasting Modification, *J. Biomed. Mater. Res. B.*, 2012, **100**(7), p 1721–1728. https://doi.org/10.1002/jbm.b.32738
26. Z. Deng, B. Yin, W. Li, J. Liu, J. Yang, T. Zheng, D. Zhang, H. Yu, X. Liu and J. Ma, Surface Characteristics of and in vitro Behavior of Osteoblast-Like Cells on Titanium with Nanotopography Prepared by High-Energy Shot Peening, *Int. J. Nanomedicine*, 2014, **9**(1), p 5565–5573. https://doi.org/10.2147/IJN.S71625
27. F. Zhou, L. Yuan, H. Huang and H. Chen, Phenomenon of "Contact Guidance" on the Surface with Nano-Micro-Groove-Like Pattern and Cell Physiological Effects, *Chinese Sci. Bull.*, 2009, **54**, p 3200–3205. https://doi.org/10.1007/s11434-009-0366-1
28. S. Minagar, J. Wang, C.C. Berndt, E.P. Ivanova and C. Wen, Cell Response of Anodized Nanotubes on Titanium and Titanium Alloys, *J. Biomed. Mater. Res. A*, 2013, **101**(9), p 2726–2739. https://doi.org/10.1002/jbm.a.34575
29. W.E. Yang and H.H. Huang, Improving the Biocompatibility of Titanium Surface Through Formation of a TiO_2 Nano-mesh Layer, *Thin Solid Films*, 2010, **518**(24), p 7545–7550. https://doi.org/10.1016/j.tsf.2010.05.045
30. M.J. Dalby, M.O. Riehle, D.S. Sutherland, H. Agheli and A.S.G. Curtis, Changes in Fibroblast Morphology in Response to Nano-Columns Produced by Colloidal Lithography, *Biomaterials*, 2004, **25**(23), p 5415–5422. https://doi.org/10.1016/j.biomaterials.2003.12.049

31. R. Olivares-Navarrete, S.L. Hyzy, M.E. Berg, J.M. Schneider, K. Hotchkiss, Z. Schwartz and B.D. Boyan, Osteoblast Lineage Cells can Discriminate Microscale Topographic Features on Titanium-Aluminum-Vanadium Surfaces, *Ann. Biomed. Eng.*, 2014, **42**(12), p 2551–2561. https://doi.org/10.1007/s10439-014-1108-3
32. R.A. Gittens, R. Olivares-Navarrete, T. McLachlan, Y. Cai, S.L. Hyzy, J.M. Schneides, Z. Schwartz, K.H. Sandhage and B.D. Boyan, Differential Responses of Osteoblast Lineage Cells to Nanotopographically-Modified, Microroughened Titanium–Aluminum–Vanadium Alloy Surfaces, *Biomaterials*, 2012, **33**(35), p 8986–8994. https://doi.org/10.1016/j.biomaterials.2012.08.059
33. L.M. Antonini, A.G.S. Junior, G. Reilly and C.F. Malfatti, Human Embryonic Stem Cell-Derived Mesenchymal Progenitor (hESCs-MP) Growth on Nanostructured Ti6Al4V Surfaces, *Mater. Res.*, 2018, **21**(5), p 1–10. https://doi.org/10.1590/1980-5373-mr-2017-1081
34. L. Bárdos and H. Baránková, Cold Atmospheric Plasma: Sources, Processes, and Applications, *Thin Solid Films*, 2010, **518**, p 6705–6713. https://doi.org/10.1016/j.tsf.2010.07.044
35. A. Cunha, A.P. Serro, V. Oliveira, A. Almeida, R. Vilar and M.-C. Durrieu, Wetting Behaviour of Femtosecond Laser Textured Ti-6Al-4V Surfaces, *Appl. Surf. Sci.*, 2013, **265**, p 688–696. https://doi.org/10.1016/j.apsusc.2012.11.085
36. D.-Z. Cui, K.-D. Park, K.-K. Lee, Y.-S. Jung, B.-A. Lee, Y.-J. Lee, O.-S. Kim, H. Chung and Y.-J. Kim, Surface Characteristics and Osteoblastic Cell Response to Titanium–8tantalum–3neobium Alloy, *Appl. Surf. Sci.*, 2012, **262**, p 107–109. https://doi.org/10.1016/j.apsusc.2012.02.112
37. M.L. Wang, R. Tuli, P.A. Manner, P.F. Sharkey, D.J. Hall and R.S. Tuan, Direct and Indirect Induction of Apoptosis in Human Mesenchymal Stem Cells in Response to Titanium Particles, *J. Orthop. Res.*, 2003, **21**(4), p 697–707. https://doi.org/10.1016/S0736-0266(02)00241-3
38. M.L. Wang, L.J. Nesti, R. Tuli, J. Lazatin, K.G. Danielson and P.F. Sharkey, Titanium Particles Suppress Expression of Osteoblastic Phenotype in Human Mesenchymal Stem Cells, *J. Orthop. Res.*, 2002, **20**(6), p 1175–1184. https://doi.org/10.1016/S0736-0266(02)00076-1
39. E.V. Ortega, A. Jos, A.M. Cameán, J.P. Mourelo and J.J.S. Egea, In vitro Evaluation of Cytotoxicity and Genotoxicity of a Commercial Titanium Alloy for Dental Implantology, *Mutat. Res.*, 2010, **702**(1), p 17–23. https://doi.org/10.1016/j.mrgentox.2010.06.013
40. T. Rae, The Toxicity of Metals used in Orthopaedic Prostheses. An Experimental Study Using Cultured Human Synovial Fibroblasts, *J. Bone Joint Surg. Br.*, 1981, **63-B**(3), p 435–440. https://doi.org/10.1302/0301-620X.63B3.7263760
41. M. Esposito, J.M. Hirsch, U. Lekholm and P. Thomsen, Biological Factors Contributing to Failures of Osseointegrated Oral Implants (II) Etiopathogenesis, *Eur. J. Oral Sci.*, 1998, **106**(3), p 721–764. https://doi.org/10.1046/j.0909-8836.t01-6-.x
42. Y. Okazaki, S. Rao, I. Yoshumasa and T. Tateishi, Corrosion Resistance, Mechanical Properties, Corrosion Fatigue Strenght and Cytocompatibility of New Ti Alloys Without Al and V, *Biomaterials*, 1998, **19**(13), p 1197–1215. https://doi.org/10.1016/S0142-9612(97)00235-4
43. H.-H. Huang, C.-P. Wu, Y.-S. Sun and T.-H. Lee, Improvements in the Corrosion Resistance and Biocompatibility of Biomedical Ti-6Al-7Nb Alloy using an Electrochemical Anodization Treatment, *Thin Solid Films*, 2013, **528**, p 157–162. https://doi.org/10.1016/j.tsf.2012.08.063
44. S. Sista, A. Nouri, Y. Li, C. Wen, P.D. Hodgson and G. Pande, Cell Biological Responses of Osteoblasts on Anodized Nanotubular Surface of a Titanium-Zirconium Alloy, *J. Biomed. Mater. Res. A*, 2013, **101**(12), p 3416–3430. https://doi.org/10.1002/jbm.a.34638
45. E.B. Partida, A.M. Ulloa, B.V. Salas, C. Velasquillo, M. Carrillo, A. Escamilla, E. Valdez and F. Villarreal, Improved Osteoblast and Chondrocyte Adhesion and Viability by Surface-Modified Ti6Al4V Alloy with Anodized TiO_2 Nanotubes Using a Super-Oxidative Solution, *Materials*, 2015, **8**(3), p 867–883. https://doi.org/10.3390/ma8030867
46. M.S. Stan, I. Memet, C. Fratila, E. Krasicka-Cydzik, I. Roman and A. Dinischiotu, Effects of Titanium-Based Nanotube Films on Osteoblast Behavior in vitro, *J. Biomed. Mater. Res. A*, 2015, **103**(1), p 48–56. https://doi.org/10.1002/jbm.a.35148
47. I. Han, B. Vagaska, H.J. Seo, J.K. Kang, B.J. Kwon, M.H. Lee and J.C. Park, Promoted Cell and Material Interaction on Atmospheric Pressure Plasma Treated Titanium, *Appl. Surf. Sci.*, 2012, **258**, p 4718–4723. https://doi.org/10.1016/j.apsusc.2012.01.065
48. D.F. Williams, E.J.C. Kellar, D.A. Jesson and J.F. Watts, Surface Analysis of 316 Stainless Steel Treated with Cold Atmospheric Plasma, *Appl. Surf. Sci.*, 2017, **403**, p 240–247. https://doi.org/10.1016/j.apsusc.2017.01.150
49. A.J. Moreira, R.D. Mansano, T.J.A. Pinto, R. Ruas, L.S. Zambon, M.V. Silva and P.B. Verdonck, Sterilization by Oxygen Plasma, *Appl. Surf. Sci.*, 2004, **235**, p 151–155. https://doi.org/10.1016/j.apsusc.2004.05.128
50. H. Wang, B. Zhao, C. Liu, C. Wang, X. Tan and M.A. Hu, A Comparasion of Biocompatibility of a Titanium Alloy Fabricated by Electron Beam Melting and Selective Laser Melting, *PLoS ONE*, 2016, **11**(7), p 1–19. https://doi.org/10.1371/journal.pone.0158513
51. T. Han, B. Chang, X. Ding, G. Yue, W. Song, H. Tang, L. Jia, L. Zhao and Y. Zhang, Improved Bone Formation and Ingrowth for the Additively Manufactured Porous Ti6Al4V Bone Implants with Strontium Laden Nanotube Array Coating, *RSC Adv.*, 2016, **6**(17), p 13686–13697. https://doi.org/10.1039/C5RA20370H
52. G.S. Stein, J.B. Lian, A.J. Van Wijnen, J.L. Stein, M. Montecino, A. Javed, S.K. Zaidi, D.W. Young, J. Choi and S.M. Pockwinse, Runx2 Control of Organization, Assembly and Activity of the Regulatory Machinery for Skeletal Gene Expression, *Oncogene*, 2004, **23**(24), p 4315–4329. https://doi.org/10.1038/sj.onc.1207676
53. M. Mozetic, A. Vesel, G. Primc, C.E. Sittner, J. Bauer, A. Eder, G.H.S. Schmid, D.N. Ruzic, Z. Ahmed, D. Barker, K.O. Douglass, S. Eckel, J.A. Fedchak, J. Hendricks, N. Klimov, J. Ricker, J. Scherschligt, J. Stone, G. Strouse, I. Capan, M. Buljan, S. Milosevic, C. Teichnert, S.R. Cohen, A.G. Silva, M. Lehocky, P. Humpolicek, C. Rodrigues, J.H. Montelongo, D. Mercier, M.M. Silvan, G. Geccone, A. Galtayries, K.S. Kleinschek, I. Petrov, J.E. Greene, J. Avila, C.Y. Chen, B.C. Munoz, H. Yi, A. Boury, S. Lorcy, M.C. Asensio, J. Bredin, T. Gans, D.O. Connell, J. Brendin, F. Reniers, A. Vincze, M. Anderle and L. Montelius, Recent Developments in Surface Science and Engineering, Thin Films, Nanoscience, Biomaterials, Plasma Science, and Vacuum Technology, *Thin Solid Films*, 2018, **660**, p 120–160. https://doi.org/10.1016/j.tsf.2018.05.046
54. K.S. Brammer, S. Oh, C.J. Cobb, L.M. Bjursten, H. Van De Heyde and S. Jin, Improved Bone-Forming Functionality on Diameter-Controlled TiO_2 Nanotube Surface, *Acta Biomater.*, 2009, **5**(8), p 3215–3223. https://doi.org/10.1016/j.actbio.2009.05.008
55. B.D. Boyan, R. Batzer, K. Kieswetter, Y. Liu, D.L. Cochran, S. Szmuckler-Monclers, D.D. Dean and Z. Schwartz, Titanium Surface Roughness Alters Responsiveness of MG63 Osteoblastic-like Cells to 1alpha,25-(OH)2D3, *J. Biomed. Mater. Res.*, 1998, **39**(1), p 77–85. https://doi.org/10.1002/(sici)1097-4636(199801)39:1%3c77::aid-jbm10%3e3.0.co;2-l
56. B.D. Boyan, S. Lossdorfer, L. Wang, G. Zhao, C.H. Lohmann, D.L. Cochran and Z. Schwartz, Osteoblasts Generate an Osteogenic Microenvironment when Grown on Surfaces with Rough Microtopographies, *Eur. Cell Mater.*, 2003, **6**(22), p 22–27. https://doi.org/10.22203/ecm.v006a03